Supplementary Information

Dynamic dissipative solitons in nematics with positive anisotropies

*Yuan Shen, Ingo Dierking**

Department of Physics, School of Natural Sciences, University of Manchester, Oxford Road, Manchester M13 9PL, UK

* Author for correspondence: ingo.dierking@manchester.ac.uk

Experimental Section

Materials. The nematics used are E7 (Xianhua, China) and 5CB (Fluorochem), respectively. The CLC with pitch $p \sim 5$ μm is made by doping a chiral dopant S811 (ZLI-811, Xianhua, China) into E7. The helical twisting power (HTP) of S811 to E7 is ~ -10.9 μm^{-1} [1], and the concentration of S811 and E7 are 1.83 wt% and 98.17 wt%, respectively. In the photoalignment process, a 0.3 % solution of SD1 (Dai-Nippon Ink and Chemicals, Japan) in dimethylformamide (DMF) is used. Silica microparticles with a monodisperse diameter of 3 μm are used in the particle trapping and cargo-transport experiments. The PVA solution is made of 0.5 wt% PVA (Aldrich) and 99.5 wt% deionized water.

Cell preparation. The cells for photoalignment are made with two ITO coated glass substrates. The substrates were cleaned in an ultrasonic bath, plasma cleaned and spin-coated with SD1. They were assembled using 10 μm spacers. The thicknesses of the cells, d, are measured by the thin film interference method [2], which vary from d = 8.6 μm to d = 14.7 μm. During the photoalignment process, the empty cells were exposed to linearly polarized ultraviolet (UV) light of wavelength λ

= 395 nm. The cell for PVA alignment was made in an analogous fashion. The ITO coated glass substrates were firstly subjected to an ultrasonic bath, plasma cleaned and spin-coated with PVA. The substrates were then unidirectionally rubbed several times with a velvet cloth. The rubbed substrates were assembled with the rubbing directions **m** being anti-parallel to each other. The cell gap was measured to be d = 9.7 μm. Finally, either nematics or CLC were heated into the isotropic phase and filled into the cells by capillary action.

Generation of solitons. The samples were heated to 50 °C (E7, both nematic and CLC) or 30 °C (5CB) by a hot stage (LTSE350, Linkam) controlled by a temperature controller (TP 94, Linkam). An AC field was applied across samples by a waveform generator (33220A, Agilent) and a home-built power amplifier.

Optical characterization. Samples were observed through a polarising optical microscope (Leica OPTIPOL) equipped with a digital camera (UI-3360CP-C-HQ, uEye Gigabit Ethernet) with tunable frame rate from 10 fps to 100 fps.

Threshold measurement. The thresholds of the solitons (E_{N} and E_{CLC}) are measured as discussed below. A region (770 μm * 409 μm) in the center of a sample was observed through POM. An AC field was applied across the sample and increased gradually (~ 0.02 V μm^{-1} per 30 s) from an amplitude E which is far below the generation threshold of the solitons. The threshold is determined as that electric field amplitude E, at which solitons can first be distinguished through POM.

Velocity measurement. The velocity of the solitons in nematics was analyzed by an open-source software ImageJ and its plugin TrackMate. At the same electric field, the velocities of over 100 solitons were automatically measured. However, the solitons in CLCs cannot be distinguished well by the software due to the low contrast with respect to the background. So their velocities were measured manually and the error bars are determined from the deviation of velocities of 5 to 10 different solitons at the same electric field.

Calculation of the polar tilted angle of mid-layer director, θ_m. The calculation of θ_m is based on the electrically controlled birefringence effect (ECB) of nematics [3]. Firstly, the dependence of the transmitted light intensity, I_a, on E (Supplementary Figure 1a) is measured by a programmed LCR meter E4980A (Agilent). The sample is placed between crossed polarizers and rotated by an angle ($\beta \sim 45$ °) with **m** deviated from the polarizer. A sinusoidal AC field (f = 5 KHz) is applied across the sample which increases automatically from 0.05 V to 16.0 V in steps of 0.025 V (0.05 V to 3.0 V) and 0.5 V (3.0 V to 16.0 V). Monochromic light (λ = 633 nm) is transmitted through the sample and polarizers and the intensity I_a is recorded by a photo-diode detector. The light intensity before the Freedericksz transition is recorded and represented as I_{a0}.

Then a low-frequency sinusoidal AC field is applied across the sample ($E \sim 0.7$ V μm^{-1}, f = 10 Hz) by a waveform generator (33220A, Agilent) and a home-built amplifier. Monochromic light (λ = 633 nm) is transmitted through the sample and the intensity (gray value), g, of a region with no solitons is recorded by a CCD camera. The intensity (gray value) at E = 0 V μm^{-1} is also recorded and symbolized as g_0. The intensity is then normalized as I_c (Supplementary Figure 1c)

$$I_c = \frac{g}{g_0} \times I_{a0} \qquad (1)$$

The simulation of the dependence of transmitted light intensity on polar tilted angle, θ(z), is based on the calculation as discussed below. To simplify the calculation, we assume that θ(z) is independent on z, i.e. θ(z) = θ_m. The extraordinary and ordinary refractivity of E7 corresponding to wavelength λ = 633 nm at 50 °C is $n_e \sim 1.69$, $n_o \sim 1.52$ [4]. Cell gaps are d = 10.1 μm for the SD1 coated cell and d = 9.5 μm for the polyimide coated cell. In the initial position **n** is orientated along the x-axis and the nematic layers manifest a birefringence of $\Delta n = n_e - n_o \sim 0.17$. When the field exceeds the Freedericksz threshold value, **n** deviates from its orientation along the x-axis, while remaining perpendicular to the y-axis. As a result, n_o remains unchanged, but n_e decreases. The relationship between n_e and θ_m can be represented as

$$n_e^{'} = \frac{n_e n_o}{(n_e^2 \sin^2 \theta_{\mathrm{m}} + n_o^2 \cos^2 \theta_{\mathrm{m}})^{1/2}} \quad (2)$$

And the phase difference between the transmitted extraordinary and ordinary ray for monochromatic light of wavelength λ is found as

$$\Delta \psi' = \frac{2\pi d(n_e^{'} - n_o)}{\lambda} = \frac{2\pi d \Delta n^{'}}{\lambda} \quad (3)$$

The transmitted light intensity depends on β and can be represented as

$$I' = I_{in} \sin^2 2\beta \sin^2 \frac{\Delta \psi'}{2} \quad (4)$$

where I_{in} is the incident polarized light intensity. The intensity is then normalized as I_{b} (Supplementary Figure 1b)

$$I_{\mathrm{b}} = \frac{I'}{I_{in} \sin^2 2\beta \sin^2 (\frac{n_e - n_o}{2})} \times I_{\mathrm{a0}} \quad (5)$$

By comparing the electric field amplitude E in Supplementary Figure 1a and 1c, we know that the oscillation dependences in Supplementary Figure 1c are located in the range after the third peak of the dependences in 1a. And the polar tilted angle, θ_{m}, can then be estimated by fitting the maximum and minimum I_{c} in Supplementary Figure 1c to 1b.

Azimuthal surface anchoring measurement. The azimuthal anchoring of E7 in the photoaligned cell is measured by the method described in refs. [5,6]. Two glass substrates coated with SD1 are uniformly photoaligned and assembled with a 90 ° twist. The sample is placed between two crossed polarizers and heated up to the isotropic phase to measure the minimum transmitted light intensity (wavelength λ = 590 nm), $I_{0\perp}$. Then one of the polarizers is rotated by 90 ° to measure the maximum intensity, $I_{0//}$. Subsequently, the sample is cooled to room temperature into the nematic phase, and the light intensity, I_t, transmitted through the sample and a pair of parallel polarizers is measured when gradually rotating the sample. Then the intensity, I_t, is normalized as

$$I = \frac{I_t - I_{0\perp}}{I_{0P}} \tag{6}$$

A typical angular dependence of the normalized transmitted intensity, I, is shown in Supplementary Figure 6a. for a cell of thickness d = 6.3 μm. For samples with different thicknesses, the minimum, I_{Min}, and maximum I_{Max}, normalized transmitted intensity are

$$I_{Min} = [\cos\tau\cos\upsilon + \frac{1}{\sqrt{1+X^2}}\sin\tau\sin\upsilon]^2 \tag{7}$$

$$I_{Max} = [\cos\tau\cos\upsilon + \frac{1}{\sqrt{1+X^2}}\sin\tau\sin\upsilon]^2 + [\frac{X}{\sqrt{1+X^2}}\sin\tau]^2 \tag{8}$$

where υ is the director twist between the top and the bottom plates, $X = \Delta\psi/(2\upsilon)$ and $\Delta\psi = 2\pi\Delta n d/\lambda$ is the phase retardation, $\tau = \upsilon(1+X^2)^{1/2}$, Δn = 0.22 for E7 at 20 °C for light of wavelength λ = 590 nm [64]. By measuring I_{Min} and I_{Max} of samples of different thicknesses d, and fitting them with Equations (7) and (8), υ can be determined. Finally, the azimuthal anchoring strength W_φ can be deduced from the surface torque equation

$$W_\varphi d\cos\upsilon = 2k_{22}\upsilon \tag{9}$$

where $k_{22} \sim 10^{-11}$ J m^{-1} is the twist elastic constant of E7 [7].

References

1. S.-S. Li, Y. Shen, Z.-N. Chang, W.-S. Li, Y.-C. Xu, X.-Y. Fan and L.-J. Chen, *Applied Physics Letters*, 2017, **111**, 231109.
2. A. M. Goodman, *Appl. Opt.*, 1978, **17**, 2779-2787.

3. L. M. Blinov and V. G. Chigrinov, *Electrooptic effects in liquid crystal materials*, Springer Science & Business Media, 1996.
4. B. Bahadur, R. K. Sarna and V. G. Bhide, *Molecular Crystals and Liquid Crystals*, 1982, **72**, 139-145.
5. C. K. McGinn, L. I. Laderman, N. Zimmermann, H.-S. Kitzerow and P. J. Collings, *Physical Review E*, 2013, **88**, 062513.
6. C. Peng, Y. Guo, T. Turiv, M. Jiang, Q.-H. Wei and O. D. Lavrentovich, *Advanced Materials*, 2017, **29**, 1606112.
7. R. D. Polak, G. P. Crawford, B. C. Kostival, J. W. Doane and S. Žumer, *Physical Review E*, 1994, **49**, R978-R981.

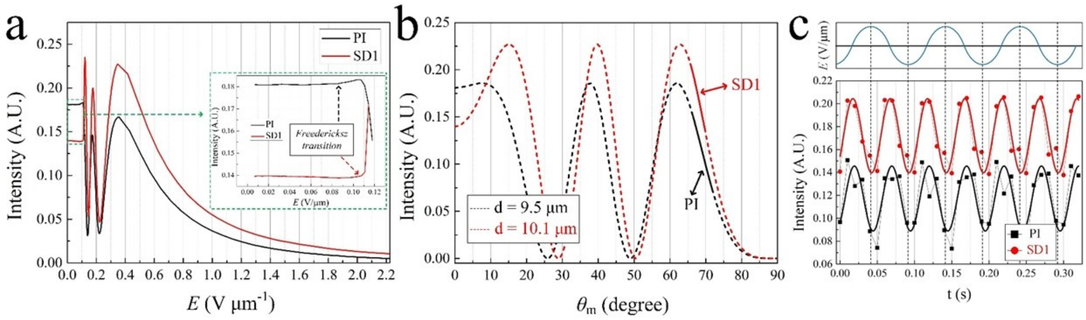

Supplementary Figure 1. Electro-optical properties of nematics. (a) Dependence of normalized transmitted light intensity (wavelength λ = 633 nm) through nematics in cells coated with polyimide (PI, black) and SD1 (red) on the amplitude of sinusoidal AC electric field, *E*. (b) Simulated dependence of normalized transmitted light intensity (λ = 633 nm) through nematics in cells with different cell gaps on the polar angle θ_m of the director. (c) Experimental measurements of normalized transmitted light intensity (λ = 633 nm) through nematics in cells coated with PI (black) and SD1 (red). $E \sim 0.7$ V μm^{-1}, $f = 10$ Hz.

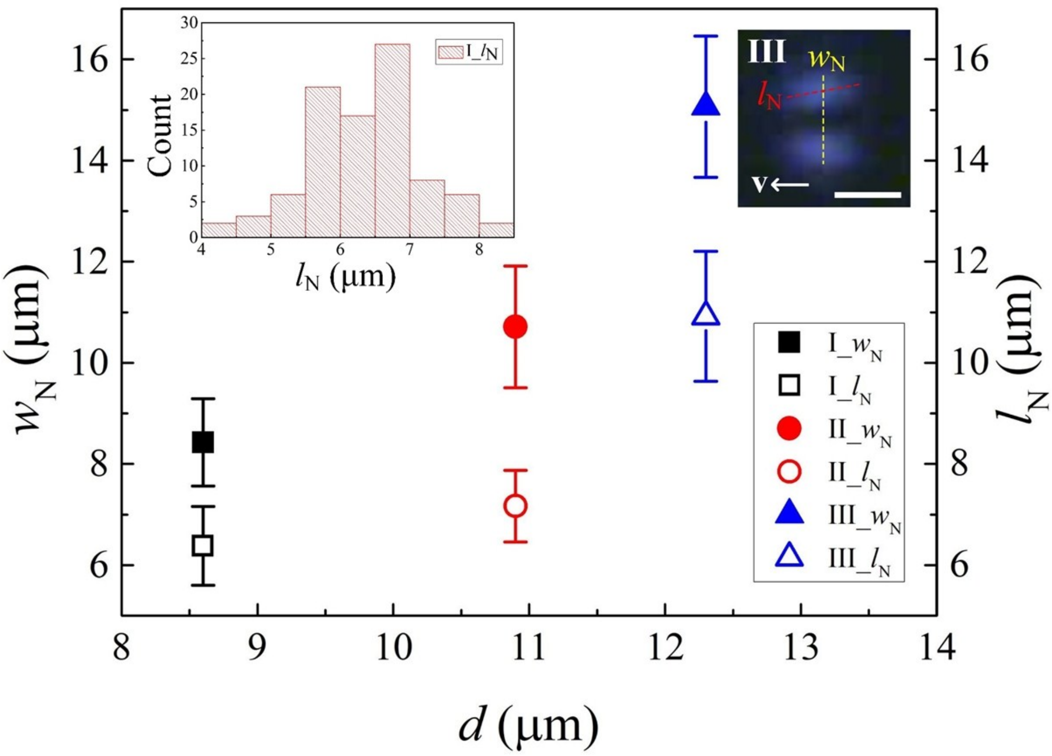

Supplementary Figure 2. Dependence of solitons' width (w_N) and length (l_N) on cell gap (d). w_N (yellow) and l_N (red) are represented in the inset (top-right corner, showing the micrograph of a soliton, scale bar 10 μm, **v** represent the velocity of the soliton). The inset on the top-left corner represents the length distribution of the solitons in case I. The applied rectangular AC field is $E \sim 1.0$ V μm^{-1}, $f = 30$ Hz. The error bars are calculated from the standard deviation of w_N and l_N of different solitons at the same conditions (electric fields and d).

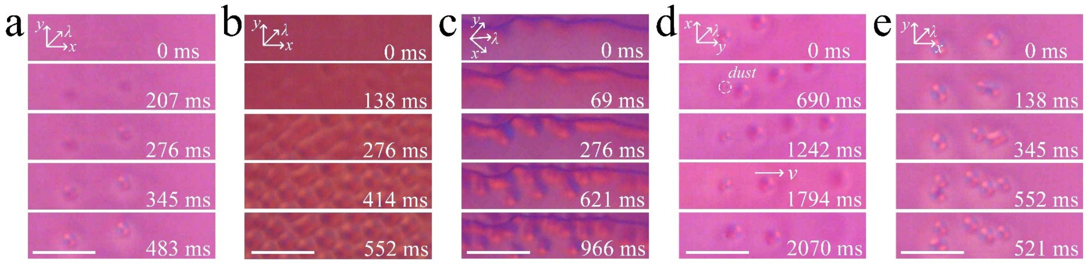

Supplementary Figure 3. Nucleation of solitons in CLCs applied with rectangular AC field. (a) solitons generate randomly in space ($E \sim 0.8$ V μm^{-1}, $f = 50$ Hz). (b) EHD flows induce solitons ($E \sim 1.0$ V μm^{-1}, $f = 50$ Hz). (c) nucleation of solitons adjacent to a disclination ($E \sim 0.9$ V μm^{-1}, $f = 60$ Hz). (d) nucleation of a soliton at a dust particle ($E \sim 1.0$ V μm^{-1}, $f = 60$ Hz). (e) proliferation of solitons ($E \sim 0.8$ V μm^{-1}, $f = 50$ Hz). **v** represents the velocity of solitons. Scale bars are 50 μm. λ represents the slow axis of the red plate. Polarizer and analyzer are parallel to the x and y axis, respectively.

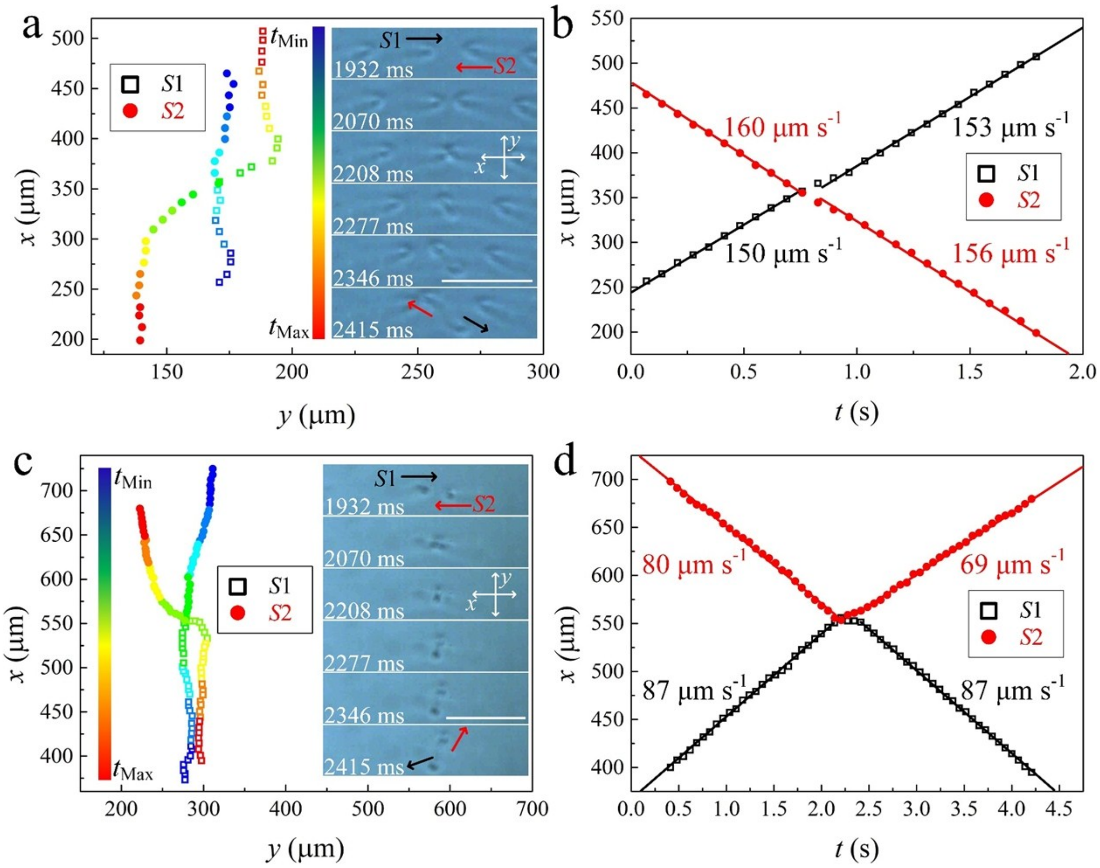

Supplementary Figure 4. Collision of solitons. (a) The trajectory of two solitons pass through each other. The color bar represents the elapsed time. $t_{\mathrm{Min}} = 0$ s, $t_{\mathrm{Max}} \sim 1.8$ s, time interval $\Delta t \sim 0.069$s. Insets are the POM micrographs of the solitons. Polarizer and analyzer are parallel to the x and y axis, respectively. The scale bar is 100 μm. The applied rectangular AC field has an amplitude of $E \sim 1.6$ V μm^{-1} and frequency $f = 60$ Hz. (b) Time dependence of x coordinates of the solitons in (a). (c) The trajectory of two solitons bump together and reflect into opposite directions. The color bar represents the elapsed time. $t_{\mathrm{Min}} = 0$ s, $t_{\mathrm{Max}} \sim 4.2$ s, time interval $\Delta t \sim 0.069$s. Insets are the POM micrographs of the solitons. Polarizer and analyzer are parallel to the x and y axis, respectively. Scale bar 100 μm. The rectangular AC field $E \sim 1.0$ V μm^{-1}, $f = 50$ Hz. (d) Time dependence of y coordinates of the solitons in (c).

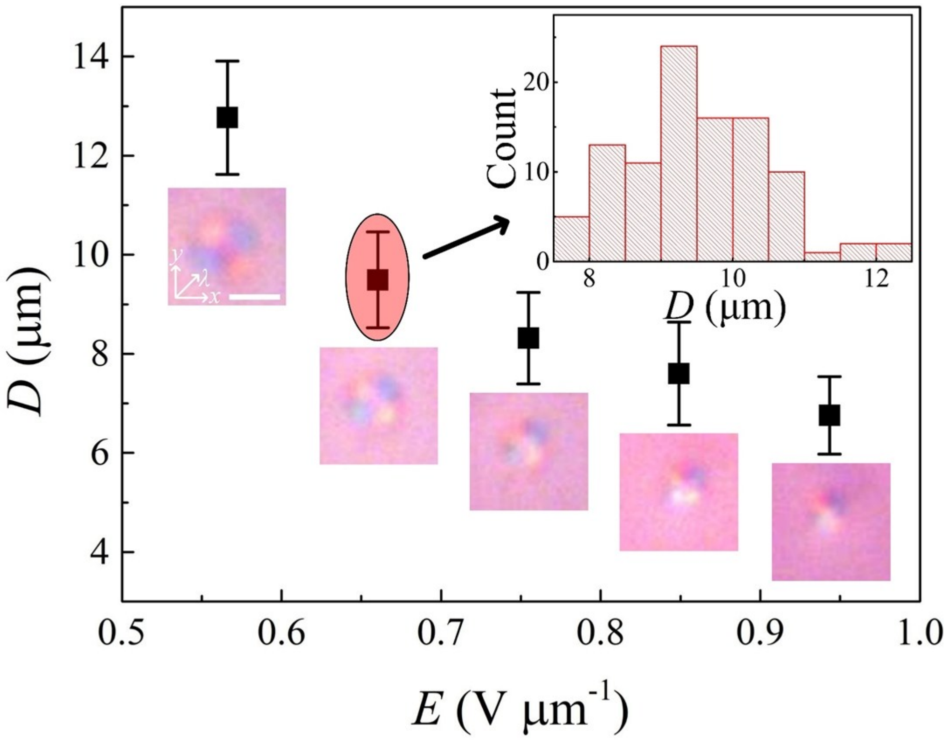

Supplementary Figure 5. Dependence of chiral solitons' diameter (*D*) on the amplitude of the applied rectangular AC electric field, *E*. The insets are the corresponding micrographs of the solitons at varied E, f = 30 Hz. d = 10.6 µm. Scale bar 10 µm. λ represents the slow axis of the red plate. Both polarizer and analyzer are parallel to the x and y axis, respectively. The inset (top-right corner) represents the diameter distribution of the soliton at $E \sim 0.66$ V µm^{-1}. The error bars are calculated from the standard deviation of diameters of different solitons at the same E.

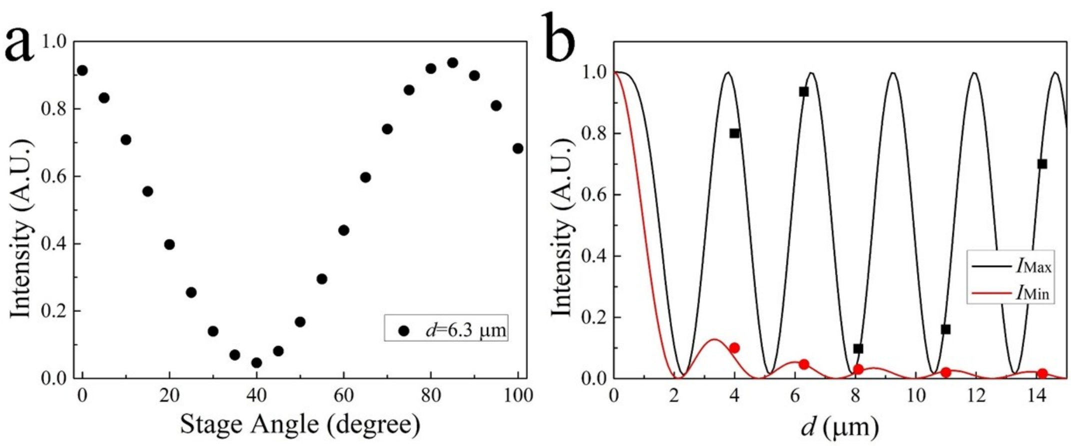

Supplementary Figure 6. Azimuthal surface anchoring of a photoaligned nematic (E7). (a) Angular dependence of the normalized transmitted light intensity (wavelength λ = 590 nm) for a cell with thickness of d = 6.3 µm, rotated between two parallel polarizers. (b) Thickness dependences of the normalized transmitted light intensities, I_{Max} (black squares) and I_{Min} (red circles). The experimental data are fitted with Equations (7) and (8) with υ ~ 83 ° (solid lines).

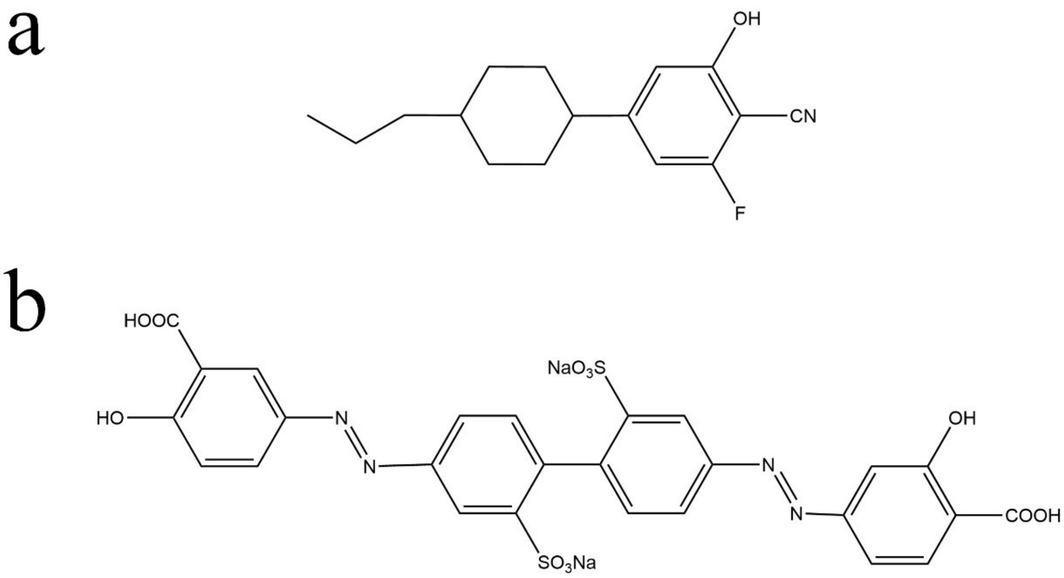

Supplementary Figure 7. Chemical structure of (a) ASE2 and (b) SD1.

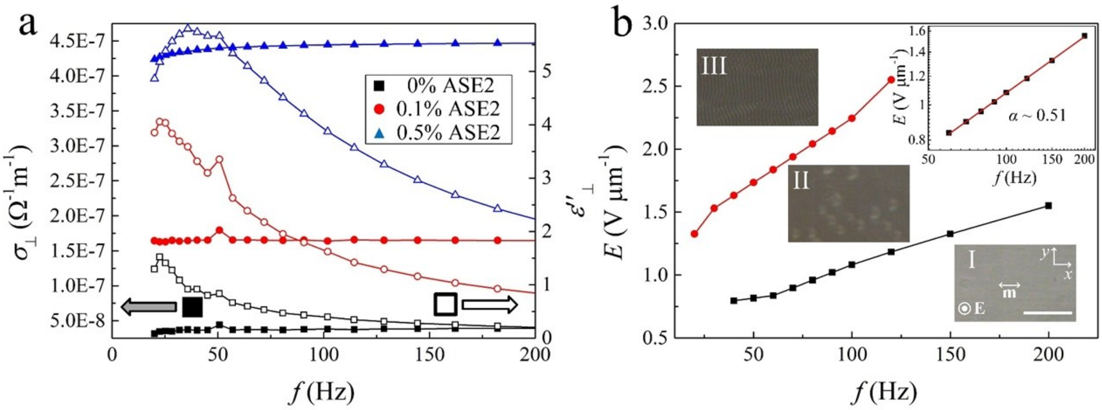

Supplementary Figure 8. Physical properties of nematics (E7) in commercial cells coated with rubbed polyimide. (a) Dependences of conductivity ($\sigma_\perp$, solid symbols) and dielectric loss ($\varepsilon_\perp$'', hollow symbols) of nematics doped with different concentrations of ionic dopant (ASE2) on frequency (*f*). (b) Threshold dependence of different states (I quasi-homeotropic state, II soliton state, III periodic EHD rolls) on the frequency of rectangular AC electric fields, *f*. Insets are the POM micrographs corresponding to different states (I: E ~ 0.6 V μm^{-1}, f = 80 Hz, II: E ~ 1.1 V μm^{-1}, f = 80 Hz, III: E ~ 2.2 V μm^{-1}, f = 80 Hz). **m** represents the alignment direction. **E** represents the electric field which is perpendicular to the *xy* plane. Both polarizer and analyzer are parallel to the *x* and *y* axis, respectively. Scale bar 100 μm. The inset on the top-right corner shows the square-root dependence of the threshold of soliton creation, E_N, on frequency. α is the slope of the dependence.

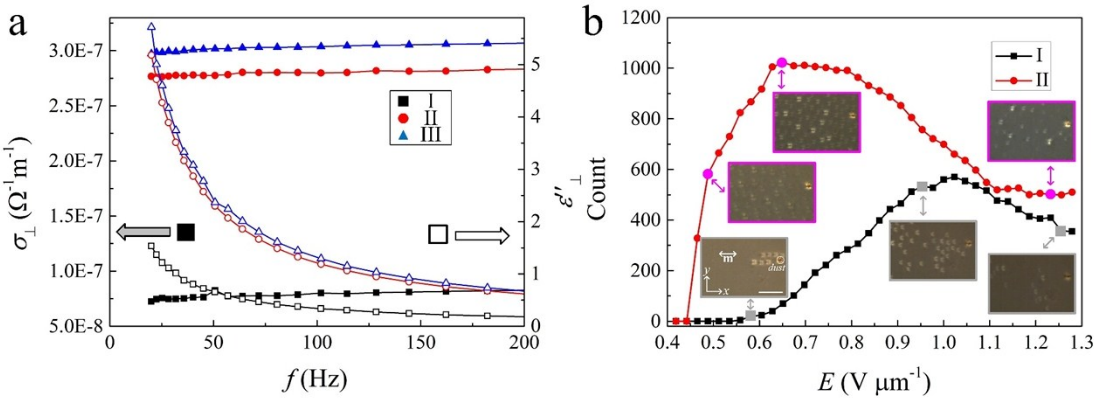

Supplementary Figure 9. Physical properties of nematics (E7) in cells coated with photoaligned SD1. (a) Dependences of conductivity ($\sigma_\perp$, solid symbols) and dielectric loss ($\varepsilon_\perp$'', hollow symbols) of nematics kept for I: 0 days, II: 3 days, III: 10 days, on frequency, f. (b) The number of solitons in a region (770 µm x 409 µm) as a function of the amplitude of rectangular AC electric field, E (I: 0day, II: 3 days, f = 20 Hz). The insets are the micrographs corresponding to different E, scale bar 50 µm, **m** represents the alignment direction; polarizer and analyzer are parallel to the x and y axis, respectively.

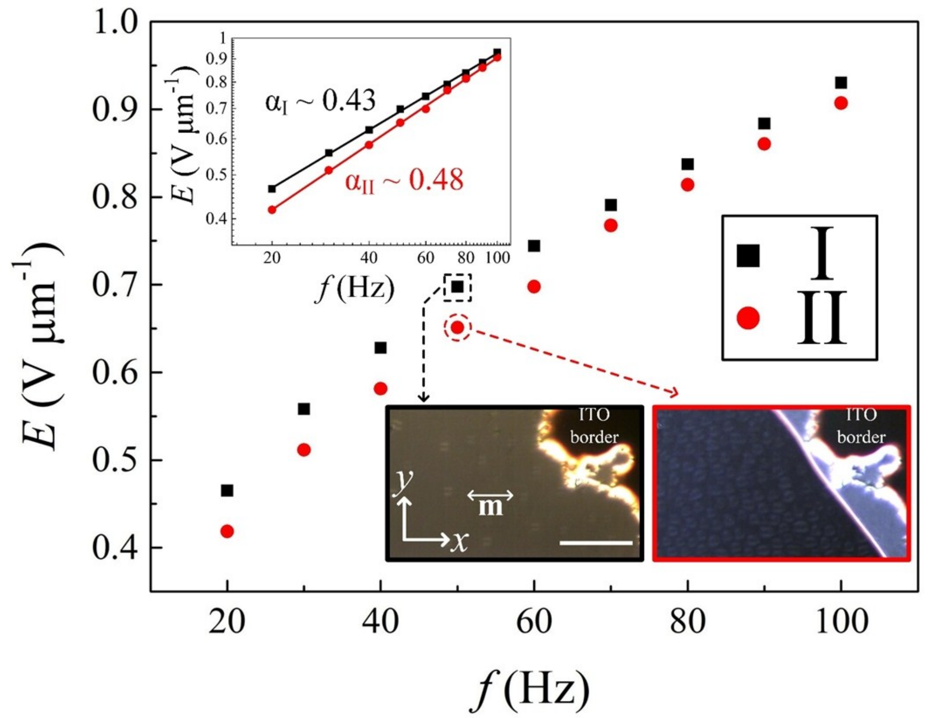

Supplementary Figure 10. Frequency dependence of the threshold of the solitons in the vicinity of the ITO electrode edge. I: 0 days, II: 3 days later. The inset (top-left) shows the square-root dependence of the threshold of soliton formation, E_N, on frequency (rectangular AC field). α is the slope of the dependence. The insets (bottom-right) are the corresponding micrographs of the solitons. scale bar 100 µm, **m** represents the alignment direction; polarizer and analyzer are parallel to the x and y axis, respectively.

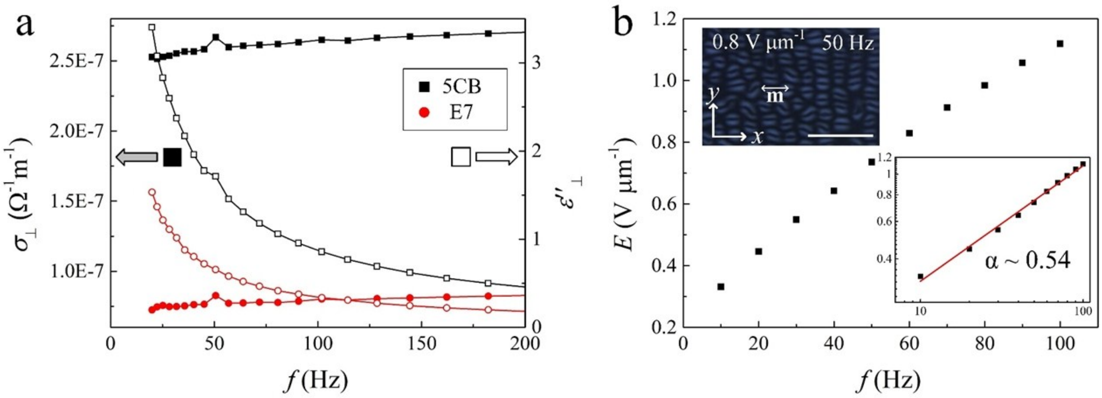

Supplementary Figure 11. Physical properties of nematics (5CB) in cells coated with photoaligned SD1. (a) Dependences of conductivity ($\sigma_{\perp}$, solid symbols) and dielectric loss ($\varepsilon_{\perp}$'', hollow symbols) of 5CB (black squares) and E7 (red circles) on frequency (*f*). (b) Frequency dependence of the threshold of solitons in 5CB (rectangular AC field). The inset (bottom-right) shows the square-root dependence of the threshold of soliton formation on frequency, α is the slope of the dependence. The inset (top-left) is a micrograph of the solitons. Scale bar 100 μm, **m** represents the alignment direction, the polarizer and analyzer are parallel to the *x* and *y* axis, respectively.

Supplementary Movies

Supplementary Movie 1. Motion of solitons in a nematic LC (NLC) and a CLC at different electric fields.

Supplementary Movie 2. Generation of solitons in NLCs. (i) random generation of solitons. (ii) EHD flows induce solitons. (iii) nucleation of solitons adjacent to a disclination. (iv) nucleation of a soliton at a dust particle. (v) proliferation of a soliton. (vi) collision of two solitons creates a new soliton.

Supplementary Movie 3. Collisions of solitons in nematic LCs at different electric fields. (i) two solitons pass through each other, (ii) two solitons collide and reflect into opposite directions.

Supplementary Movie 4. Unidirectional motion of solitons in a nematic LC driven by modulated AC field and circular motion of solitons in a CLC.

Supplementary Movie 5. Generation of solitons in CLCs. (a) random generation of solitons. (b) EHD flows induce solitons. (c) nucleation of solitons adjacent to a disclination. (d) nucleation of a soliton at a dust particle. (e) proliferation of solitons.

Supplementary Movie 6. Collisions of solitons in CLCs at different electric fields. (i) two solitons pass through each other, (ii) two solitons collide and reflect into opposite directions.

Supplementary Movie 7. Cargo transport and patterned photoalignment. (a) micro-particle trapping by solitons. (b) micro-particle transport by a soliton. (c) propagation of solitons in regions with different alignment directions.

Supplementary Movie 8. (a) Solitons in a cell coated with rubbed PVA and (b) solitons at the ITO edges of a commercial cell.